Available online at www.CivileJournal.org

Civil Engineering Journal

(E-ISSN: 2476-3055; ISSN: 2676-6957)

Vol. 12, No. 03, March, 2026

Rainfall-Induced Stability of Reinforced Slopes with Twin Parallel Tunnels: Experimental Validation and Coupled Hydro-Mechanical Analysis

Zaid S. Alajlan [1], Loujain Suliman [2*], Hamzah M. B. Al-Hashemi [3], Ali Alatify [1]

[1] *Department of Civil Engineering, College of Engineering in Al-Kharj, Prince Sattam Bin Abdulaziz University, Al-Kharj,11942, Saudi Arabia.*

[2] *State Key Laboratory of Coal Mine Disaster Dynamics and Control, China Chongqing University, Chongqing 400044, China.*

[3] *Indian Institute of Technology Bombay, Powai, Mumbai 400076, Maharashtra, India.*

Received 02 December 2025; Revised 19 February 2026; Accepted 24 February 2026; Published 01 March 2026

Abstract

Climate change has increased the frequency and intensity of extreme rainfall events, which significantly threatens slope stability by elevating pore-water pressure, reducing effective stress, and weakening soil strength. This study aims to investigate the rainfall-induced hydro-mechanical response of a fill slope containing twin parallel tunnels and to evaluate the effectiveness of reinforcement measures in improving slope stability under such conditions. A combined experimental–numerical approach was adopted. First, a physical model test of twin tunnels excavated within a slope was conducted to provide validation data for the numerical model. Subsequently, a parametric numerical analysis was performed using the finite element method implemented in PLAXIS 3D to simulate the coupled hydraulic–mechanical behavior of the slope–tunnel system under varying rainfall intensities and durations. Reinforcement measures, including piles and plates, were incorporated to assess their stabilizing performance. The results show that rainfall duration has a more significant influence on slope deformation and pore-water pressure than rainfall intensity. Reinforcement measures effectively reduce deformation and enhance slope stability, although they have limited influence on the overall saturation distribution. Reinforced slopes also exhibit increased total discharge due to preferential seepage along soil–structure interfaces. The novelty of this study lies in integrating physical model validation with three-dimensional coupled hydro-mechanical numerical analysis to comprehensively evaluate deformation, pore-water pressure, and seepage behavior in reinforced tunnel–slope systems under rainfall conditions.

Keywords: Rainfall; Sustainability; Reinforcement; Plaxis3D; Model Test; Fill Slope; Tunnel.

1. Introduction

Climate change has increased both the frequency and intensity of extreme rainfall events, resulting in higher pore-water pressures and a reduction in the shear strength of slope-forming soils. These effects accelerate the onset of slope failure by enhancing saturation, deteriorating the internal soil structure, and inducing instability in natural as well as engineered slopes. In order to gain a clearer understanding of this combined phenomenon, the present study focuses on the interaction between rainfall infiltration and tunneling activities and their joint influence on slope stability. A physical model incorporating twin tunnels within a fill slope was developed to replicate field conditions and assess the resulting mechanical response. To enhance stability, pile reinforcement was incorporated, and its efficiency in alleviating rainfall-induced deformation and failure was systematically examined.

* Corresponding author: lojain-s@hotmail.com

https://doi.org/10.28991/CEJ-2026-012-03-022

In recent years, extreme rainfall events have become more frequent and are now widely recognized as a major factor intensifying geohazard risks [1, 2]. In China, rainfall-induced landslides resulted in over 1,200 fatalities and more than 100 billion yuan in economic losses between 2010 and 2022 [3]. Tian et al. [4] examined the impact of extreme rainfall and drainage system failure on a deep-buried karst tunnel, demonstrating that inadequate drainage capacity significantly amplifies pore-water pressure and structural distress in underground infrastructures. Tang et al. [5] investigated water infiltration behavior in loess and examined the resulting structural response of tunnels subjected to rainfall, demonstrating that preferential flow channels significantly accelerate wetting-front progression and contribute to tunnel instability. A recent study by Qian et al. [6] examined the mechanical behavior of tunnel linings in karst regions under heavy rainfall, identifying how elevated cavity water pressures influence internal forces, deformation, and structural safety.

The tunneling and the resulting stresses and induced settlement have been studied by many researchers. Xu et al. [7] studied the variation law of surrounding rock stress and displacement caused by one tunnel excavation in a gully area. And concluded that the deformation was small in the gentle section of the gully but increased sharply in the section of slope where there was even collapse. Jiang et al. [8] made a shaking table test for twin tunnels in a slope with a sensitivity analysis. Choi & Lee [9] did a model test to evaluate the displacement and crack propagation during the excavation of a new tunnel near an existing tunnel and concluded that, depending on the size of the existing tunnel, increasing the distance between tunnel centers causes displacement around tunnels to diminish and stabilize beyond a certain distance. Kim [10] investigated the stability of asymmetrical twin tunnels constructed in rock mass; four types of test models, which had respectively different pillar widths and loading conditions, were experimented with. Seo et al. [11] studied the stability of the pillar between twin tunnels and proposed a new pillar-reinforcement technology for improved pillar stability.

Moreover, Ng & Lu [12] studied the influence of the tunnel on the displacement and stress of the ground and adjacent extended foundations and verified it with laboratory model tests and numerical simulation analysis. Chen et al. [13] and Zhao et al. [14] analyzed the impact of urban underground engineering and the potential damage to the surrounding environment by monitoring various additional stresses and ground subsidence caused by shield tunnel construction. In the case of the tunnel under-crossing the road, it is inevitable that it will disturb the roadbed slope and cause road surface subsidence [15, 16]. Kaya et al. [17] studied the influence of tunnel construction on slope displacement and stress and discussed the failure mechanism of tunnel-disturbed slopes. Fattah et al. [18] analyzed the shape of the settlement groove caused by tunnel excavation in the cohesive foundation using analytical solutions, empirical solutions, and numerical solutions.

The effect of rainfall on slope stability has been extensively investigated in recent years. Lin & Zhong [19] examined the influence of rainfall intensity and pattern on the mechanisms of slope instability and slip surface formation. Similarly, Ma et al. [20] analyzed the effect of stagnant water curves on the stability of unsaturated soil slopes. Tu et al. [21] explored the deformation behavior and control measures of slopes under rainfall infiltration through engineering case studies. In addition, several other studies have emphasized the critical role of rainfall characteristics in triggering slope failures. For example, Rahardjo et al. [22] and Ng & Shi [23] highlighted the influence of rainfall infiltration on matric suction reduction and shear strength degradation in unsaturated slopes. Furthermore, Len & Zhong [19] demonstrated that prolonged or high-intensity rainfall can significantly accelerate pore-water pressure build-up and deformation in natural and engineered slopes. These findings collectively indicate that rainfall-induced slope instability is governed by a complex interaction between hydrological, geotechnical, and environmental factors. However, in this paper the settlement induced due to excavating twin tunnels in a slope was investigated using two main methods, which are numerical simulation by using the PLAXIS3D software package. In addition, the effect of rainfall on the distribution of effective stress and pore water pressure was investigated.

The research employed two integrated approaches: a physical model test to capture realistic deformation behavior and a numerical simulation using the Finite Element Method (FEM) implemented in PLAXIS 3D. The numerical model was designed to reproduce the coupled hydro-mechanical behavior of the slope–tunnel–pile system under varying rainfall conditions. The simulation results demonstrate that when piles are installed after rainfall, the soil—already weakened and saturated—cannot effectively transfer load or resist deformation, leading to excessive settlement. Conversely, when piles are installed prior to rainfall, they provide substantial improvement in slope performance by maintaining structural integrity, minimizing settlement, and sustaining long-term stability. These findings highlight the critical importance of timely reinforcement installation in mitigating the adverse impacts of extreme rainfall on tunnel-affected slopes.

This study hypothesizes that the rainfall-induced instability of a fill slope containing twin parallel tunnels is primarily governed by coupled hydro-mechanical interactions among rainfall infiltration, pore-water pressure development, and stress redistribution around underground openings. Specifically, rainfall duration is expected to exert a greater influence on slope deformation and tunnel–soil interaction than rainfall intensity, while reinforcement measures (piles or plates) are anticipated to significantly reduce mechanical deformation without substantially altering the global hydraulic response of the slope. Despite extensive studies on rainfall-induced slope instability and tunnel–slope interaction, there remains a notable lack of comprehensive investigations that integrate physical modeling with three-dimensional coupled

hydro-mechanical numerical analysis to systematically examine the behavior of slopes containing twin parallel tunnels under rainfall conditions. In particular, existing research has largely overlooked the combined effects of reinforcement measures on both deformation control and hydrological response. While reinforcement has been shown to significantly reduce deformation, its limited influence on global saturation and its potential to increase localized discharge through preferential seepage along soil–structure interfaces remain insufficiently understood. This gap underscores the need for integrated experimental–numerical approaches capable of capturing the complex coupled mechanisms governing deformation, seepage, and reinforcement effects in tunnel–slope systems subjected to rainfall. Figure 1 shows the structure of the article.

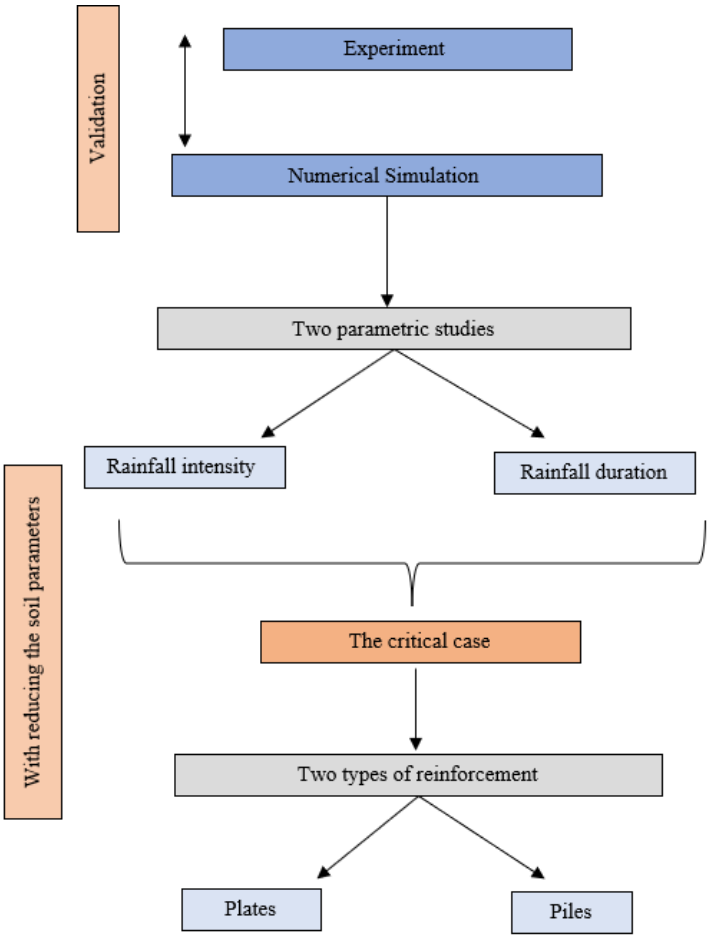

Figure 1. The structure of the study

2. The Methodological Approach

The theoretical framework of this study integrates similarity theory, unsaturated soil mechanics, and coupled hydro-mechanical analysis to investigate rainfall-induced deformation in slopes containing twin parallel tunnels. Similarity theory was applied to the physical model to ensure geometric, mechanical, hydraulic, and temporal consistency between the laboratory model and the prototype, enabling realistic reproduction of rainfall infiltration, pore-pressure evolution, and deformation processes.

2.1. Mode Test-Physical Modelling

In this stage of the study, the slope model was subjected to simulated rainfall to examine its hydraulic and mechanical response under infiltration conditions. The rainfall was applied uniformly across the slope surface using a controlled artificial rainfall system designed to reproduce natural precipitation intensity and duration at a scaled level consistent with similarity requirements. The primary objective of this phase was to observe the development of pore water pressure, deformation patterns, and potential failure mechanisms induced by rainfall infiltration.During the test, sensors were installed at different depths and sections of the slope to monitor variations in pore water pressure, displacement, and surface deformation in real time. The rainfall infiltration process caused a gradual increase in pore water pressure within the slope, leading to a reduction in effective stress and a subsequent decrease in the factor of safety. In this stage of the investigation, the rainfall event was applied after the completion of tunnel excavation. Consequently, the excavation process itself was not considered as an influencing factor in this phase of analysis. The slope and surrounding ground had already reached a post-excavation equilibrium condition prior to the initiation of rainfall. Therefore, the focus of

this stage was exclusively on evaluating the hydrological and stability response of the slope to rainfall infiltration under the existing geometric and stress conditions created by the completed tunnels. This experimental setup allows for isolating the effects of rainfall infiltration on the slope's mechanical behavior without the interference of excavation-induced stress redistribution. It provides a clear understanding of how rainfall alone influences pore water pressure development, deformation patterns, and overall stability in a slope that has already undergone structural modification due to tunneling. The model test calculation would be as the following:

For the rainfall time:

$$\frac{t\ model\ tets}{t\ numerical\ simulation} = \frac{1}{\sqrt{cl}} \tag{1}$$

For the intensity of rainfall:

$$\frac{\text{qmodel test}}{q\ numerical\ simulation} = \frac{1}{\sqrt{cl}} \tag{2}$$

The applied rainfall intensity in the prototype was set to 200 mm/day in accordance with the relevant Chinese design code, with a corresponding rainfall duration of 0.2 days, equivalent to approximately 4.8 hours. This duration was selected to simulate a short-term, high-intensity rainfall event representative of extreme precipitation conditions commonly used in slope stability and infiltration analyses. Figure 2 illustrates the procedures of the physical model test. Figure 2(a) presents the process of preparing and mixing the model materials before placing them into the model box. Figure 2(b) depicts the setup of the instrumentation, including the data acquisition sensors and the model box. Figure 2(c) displays the device employed to simulate rainfall infiltration on the slope surface. Finally, Figure 2(d) shows the complete experimental setup, including the model box integrated with the rainfall simulation system.

To ensure the reliability of the physical model test, similarity theory was applied to maintain consistency between the prototype slope–tunnel system and the scaled laboratory model. Geometric similarity was achieved by adopting a constant length scaling ratio, under which all geometric dimensions of the slope, tunnels, and reinforcement elements were proportionally reduced. Mechanical similarity was ensured by selecting model materials whose density, stiffness, and shear strength parameters satisfied the required similarity relationships with the prototype. The stress similarity ratio was controlled through the self-weight of the model materials and the imposed boundary conditions, allowing the stress distribution within the model to realistically represent that of the prototype system. Hydraulic similarity was achieved by adjusting the rainfall intensity and duration, according to the time and permeability similarity ratios. A controlled artificial rainfall system was employed to reproduce scaled precipitation conditions, ensuring that seepage paths, pore water pressure evolution, and saturation processes remained consistent with similarity requirements.

(a)

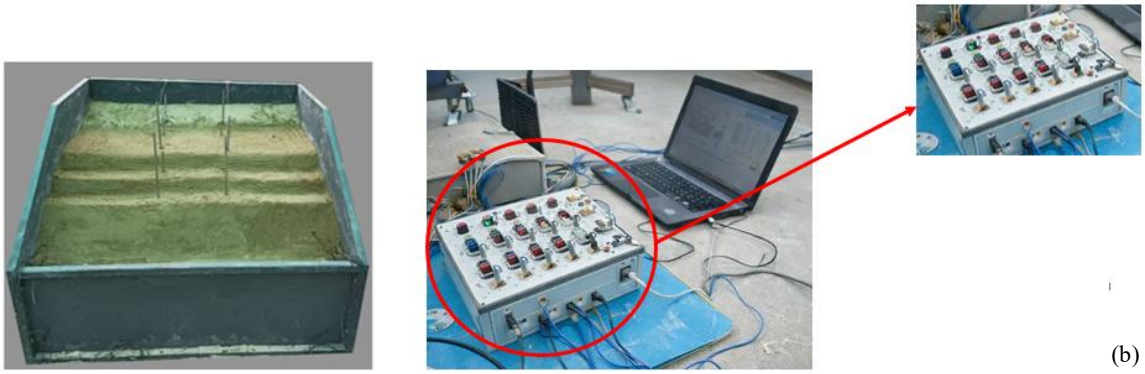

(b)

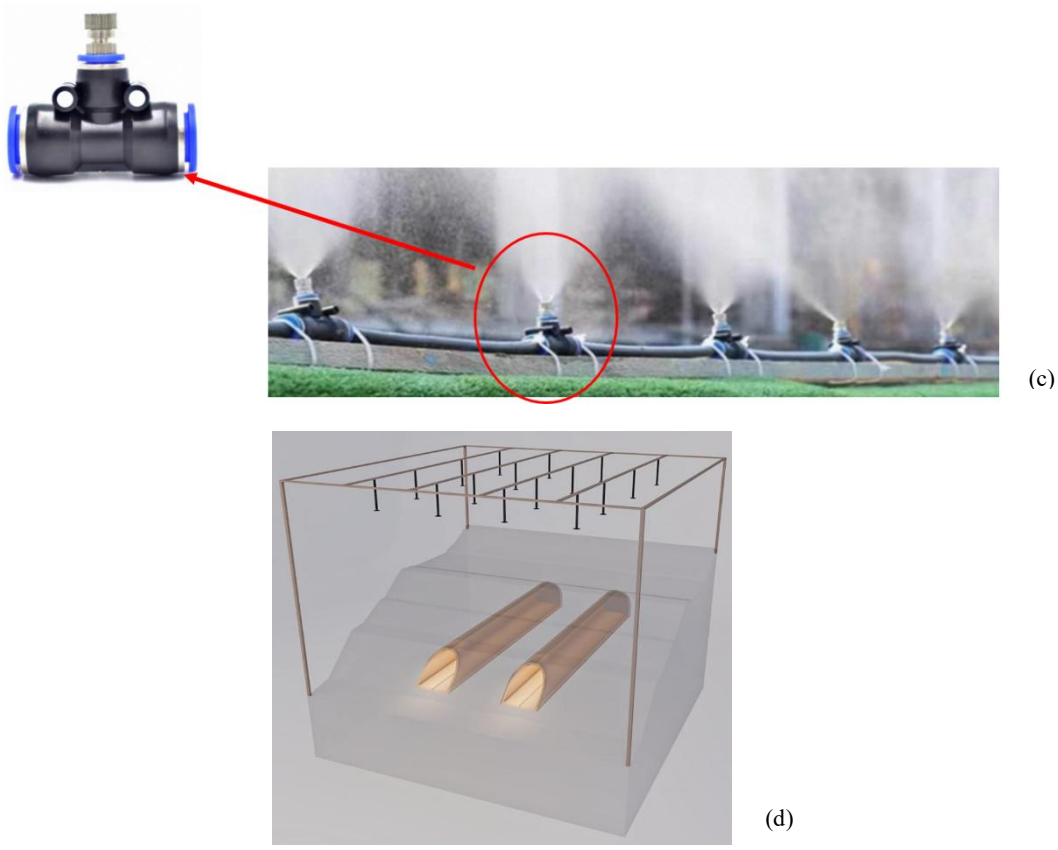

Figure 2. (a) The model test similar materials; (b) building the model test with sensors testing; (c) they used tool for rainfall and; (d) the model test design

2.2. Numerical Simulation-FEM analysis

In this numerical simulation, the rainfall condition was applied once the completion of tunnel excavation, meaning that the excavation process was not included as an active phase in this stage of the analysis. At the beginning of the rainfall simulation, the model represented the post-excavation equilibrium state, where the stress field and deformation were already stabilized following tunnel construction. By excluding the excavation process, the model isolates the influence of rainfall on pore water pressure generation, effective stress variation, and slope displacement behavior. This approach ensures that the observed responses can be attributed entirely to rainfall effects rather than to excavation-induced stress redistribution. The similarity ratio adopted for this study is 100, ensuring consistency between the prototype and the scaled model in accordance with similitude principles.

The construction process was divided into four main stages. (1) The gravity stage, which represents the initial phase, was conducted to establish the self-weight equilibrium of the slope and surrounding materials. (2) The tunnel excavation stage was then performed, during which appropriate support systems were installed to ensure structural stability. (3) The coupled analysis stage incorporated the effects of rainfall infiltration as an external condition to simulate hydro-mechanical interactions within the slope. (4) Finally, the safety analysis stage was carried out to evaluate the overall stability of the slope by determining the corresponding factor of safety. Figure 3 shows the FEM model. While, Figure 4 shows the sensors positions. The lateral boundaries of the model were constrained against horizontal movement, while the base was fully fixed in all degrees of freedom. The upper boundary was left free, allowing natural deformation under loading conditions. The distance between the tunnel edge and the model boundaries on both sides was set to 6.3 times the tunnel diameter, which is sufficiently large to eliminate boundary effects and ensure that the excavation-induced deformations do not interact with the model limits. The distance was determined based on a sensitivity analysis of the boundary conditions, supplemented by reference to relevant studies in the existing literature.

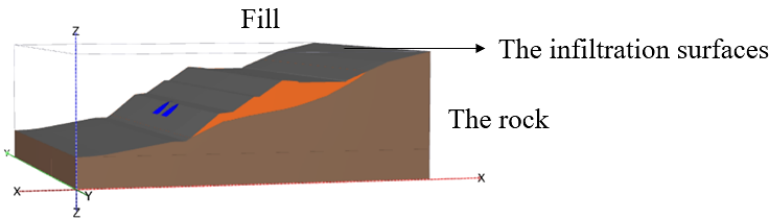

Figure 3. FEM main model

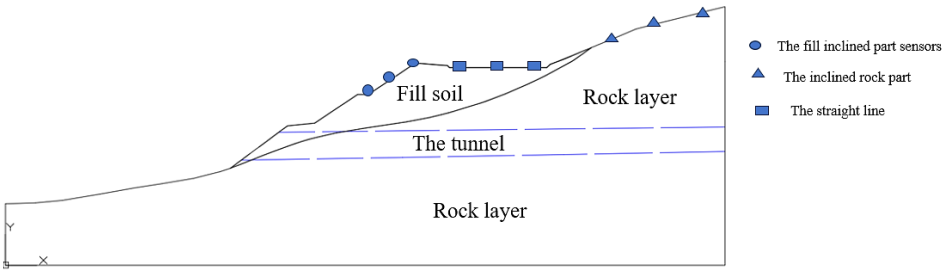

Figure 4. Sensor's position

3. Geotechnical Parameters

In this section, the geotechnical parameters used in the study are presented. The parameters adopted in the numerical simulation are listed in Table 1, while the corresponding parameters applied in the physical model test are summarized in Table 2. This comparison enables the validation of the numerical simulation results against the experimental observations under equivalent geotechnical conditions. Table 3 presents the material properties employed in the model test, all of which were selected based on the similarity material testing principles to ensure appropriate scaling between the prototype and the model. The similarity ratio, which has a value of 100, is defined by the following equation.

$$Similarity\ Ratio\ (Cl) = \frac{Numerical\ simulatoin}{Physical\ model} \quad (1)$$

Finally, Table 4 provides the details of the materials used in the proposed support system, which were designed to replicate the mechanical and structural behavior of the actual reinforcement elements under model conditions. The Mohr–Coulomb (M–C) constitutive model was adopted to represent the mechanical behavior of both the fill material and the underlying rock strata. This model was selected due to its robustness and suitability for simulating geomaterials whose shear strength is governed primarily by cohesion and internal friction. The M–C model provides a linear elastic–perfectly plastic framework that captures the essential features of soil and rock response under tunnelling-induced stress changes. Its parameters—elastic modulus, Poisson's ratio, cohesion, friction angle, and dilatancy—allow for an appropriate representation of the stress–strain behavior of both the engineered fill and the relatively stiffer rock layers. Given the objectives of this study and the available geotechnical data, the Mohr–Coulomb model offers a reasonable and computationally efficient approximation for evaluating ground deformation and tunnel stability.

Table 1. The parameters used in the numerical simulation process

	C (kN/m^2)	Φ (degree)	E (kN/m^2)	μ	γ (kN/m^3)
Fill	26	**33**	30000	0.4	18
Rock	200	**33**	2100000	0.2	24

Table 2. The reduced parameters in the numerical simulation

	C (kN/m^2)	Φ (degree)	E (kN/m^2)	μ	γ (kN/m^3)
Fill	0.26	**33**	300	0.4	18
Rock	2	**33**	21000	0.2	24

Table 3. The reduced parameters for the parametric numerical simulation

	C (kN/m^2)	Φ(degree)	E (kN/m^2)	μ	γ(kN/m^3)
Fill	10	**33**	20000	0.4	18
Rock	150	**33**	500000	0.2	24

Table 4. The piles parameters in the parametric study

	d/t (m)	E (GPa)	μ
Piles	**0.8**	30	0.2
Plates	**0.035**	200	0.2

4. Results

4.1. The Model Test Validation

Figure 5 presents the validation of numerical simulation results against experimental data in terms of excess pore water pressure along a specific section of the slope in the straight part of the slope. It can be observed that the overall trend of the numerical simulation is in good agreement with the experimental data, confirming that the numerical model can reasonably capture the pore pressure distribution along the section. The small discrepancies between the two datasets may result from several factors, such as simplifications in the boundary conditions, heterogeneity in soil properties, or measurement limitations during the physical experiment.

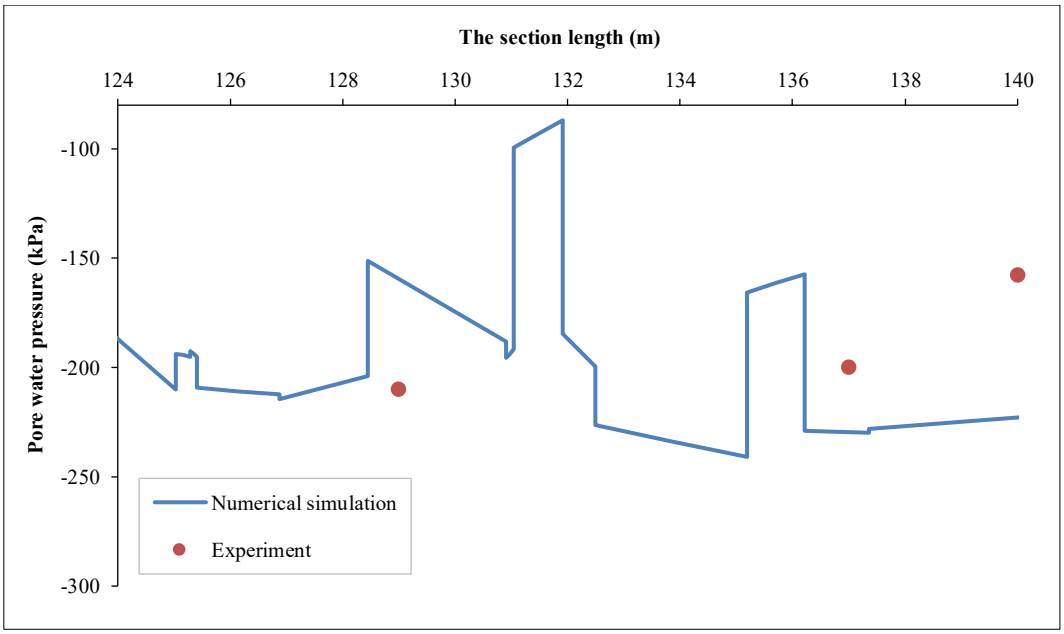

Figure 5. The straight part of the slope

Figure 6 illustrates the validation of numerical simulation results against experimental measurements of excess pore water pressure along the inclined part of the slope which located in the rock. The comparison shows that both the experimental and numerical results follow a similar overall trend, with excess pore water pressure increasing significantly at certain positions along the slope (notably between 165 m and 190 m). These peaks correspond to zones of higher rainfall infiltration and local stress concentration caused by the geometry of the slope.

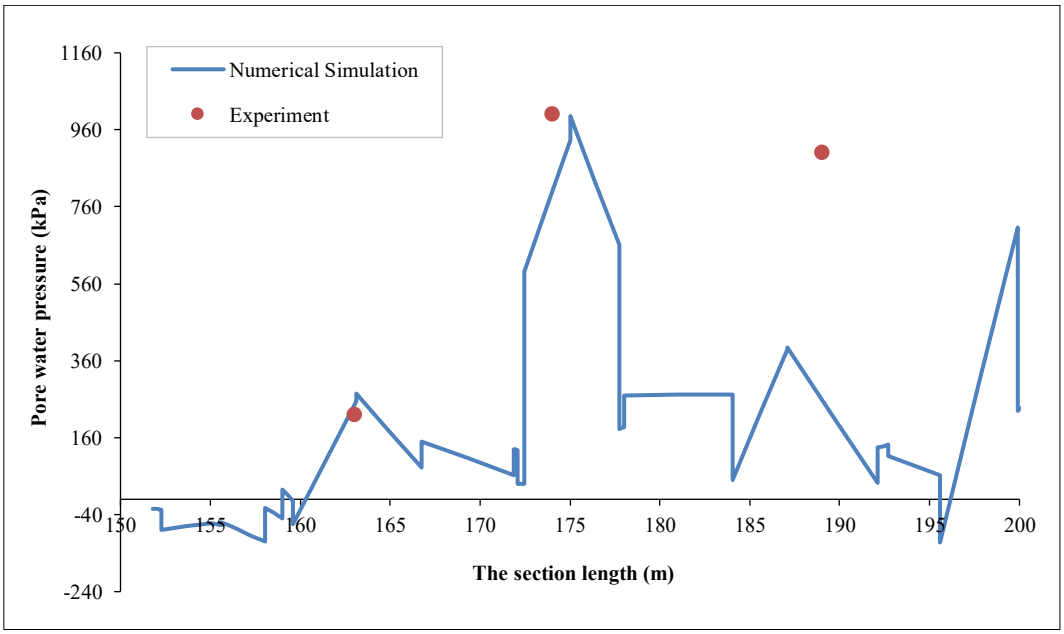

Figure 6. The inclined rock

Figure 7 presents a comparison between the numerical simulation and experimental results of excess pore water pressure along the slope section between 103 m and 117 m. The comparison indicates a generally consistent trend between experimental and numerical data. Both datasets show a gradual decrease in excess pore water pressure along the section length, reflecting the dissipation of pore pressure with distance and depth. The numerical simulation successfully captures the overall behavior and magnitude of the pore pressure distribution, with values ranging approximately between −100 and −450 kN/m², which aligns well with the experimental observations.

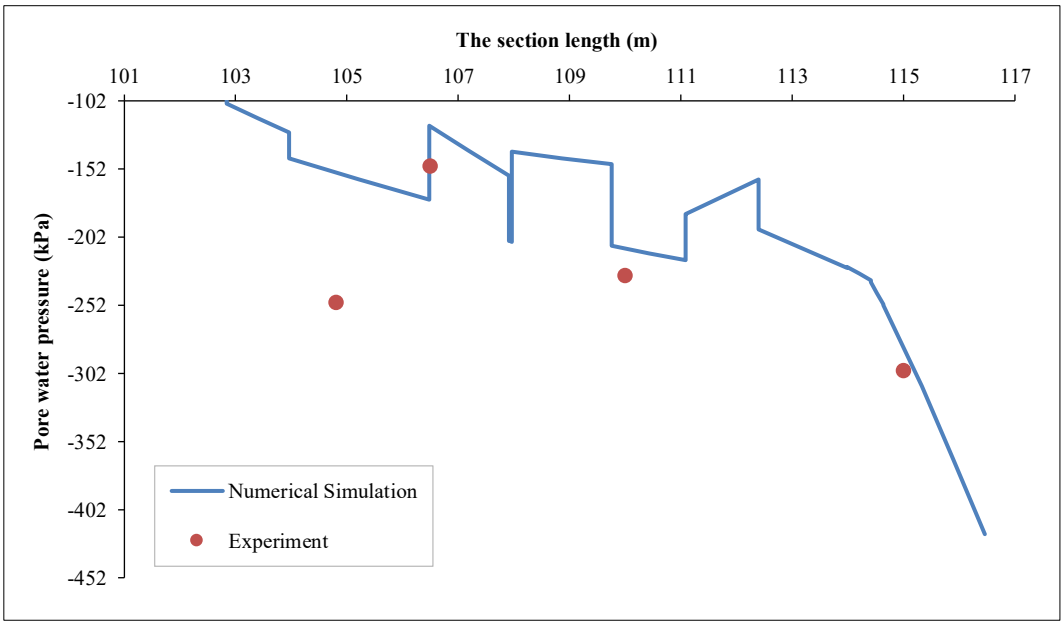

Figure 7. The inclined fill

4.2. Parametric Study

To comprehensively examine the effect of rainfall on slope behavior, the rainfall condition in this section was defined as continuous rainfall. In *PLAXIS 3D*, this configuration enables the user to specify the rainfall duration directly within the calculation phases. The rainfall intensity was assigned as a constant value to maintain a uniform precipitation rate throughout the simulation period, thereby facilitating controlled analysis of the hydromechanical response. The investigated domain corresponds to the inclined section of the slope, which is directly exposed to rainfall infiltration and thus represents the most critical zone for evaluating rainfall-induced instability and pore water pressure development. The parametric study presented in this section was conducted under a constant total rainfall quantity to isolate the effects of rainfall characteristics on slope stability. Four principal cases were examined to evaluate the influence of rainfall intensity, duration, and reinforcement measures under varying soil strength conditions. Specifically, the study addressed the following:

- The effect of rainfall intensity under high-strength soil parameters.
- The effect of rainfall duration under high-strength soil parameters.
- The slope response under low-strength soil parameters.
- The performance of the proposed reinforcement system. In this section, two types of support were used: piles and a plate with equivalent thickness

Each scenario was systematically analyzed to assess how variations in rainfall intensity and duration influence slope deformation behavior, overall stability, and the development of pore water pressure within the soil mass.

4.2.1. The Effect of the Rainfall Intensity on Fill Slope (High Strength Parameters)

In this section, various parameters of rainfall intensity were examined. Four primary rainfall intensities were considered: 100 mm/day, 200 mm/day, 300 mm/day, and 400 mm/day. The results indicate that the first three intensities (100, 200, and 300 mm/day) produce negligible differences in the observed settlement. However, when the rainfall intensity increases to 400 mm/day, the settlement rises noticeably to approximately 0.2 mm. Furthermore, the results indicate that the majority of the displacement is attributed to soil swelling, whereas settlement predominantly occurs under higher rainfall intensities. This swelling is primarily attributed to moisture-induced volumetric expansion as

partially saturated soil absorbs water, particularly in fine-grained materials. Under moderate rainfall conditions, partially saturated soils tend to exhibit volumetric swelling due to moisture absorption, whereas higher rainfall intensities and sustained infiltration lead to soil saturation, effective stress reduction, and settlement [24].

With respect to the excess pore water pressure, the findings reveal that in the inclined section of the slope exposed to rainfall infiltration, the pore water pressure at an intensity of 200 mm/day was noticeably higher compared with that at 100 mm/day. Additionally, when the rainfall intensity increased to 300 mm/day, the corresponding pore water pressure was relatively lower than that observed at 400 mm/day. This suggests that elevated rainfall intensity significantly amplifies pore water pressure within the slope, thereby influencing its overall stability and deformation behavior. This phenomenon can be attributed to the infiltration–saturation dynamics of the slope soil. At moderate rainfall intensities (e.g., 300 mm/day), the infiltration rate is close to the soil's permeability limit, allowing part of the rainfall to percolate gradually without causing full saturation. Consequently, pore water pressure remains comparatively moderate. However, when the rainfall intensity reaches 400 mm/day, the rainfall rate exceeds the soil's infiltration capacity, leading to surface ponding and rapid saturation of the near-surface layers. This excess water infiltration results in a sharp rise in excess pore water pressure within the slope body. The increase in pore pressure under such high-intensity rainfall reduces the effective stress and contributes to larger deformations or potential instability. Figure 8 shows the effect of rainfall intensity on the settlement and pore water pressure.

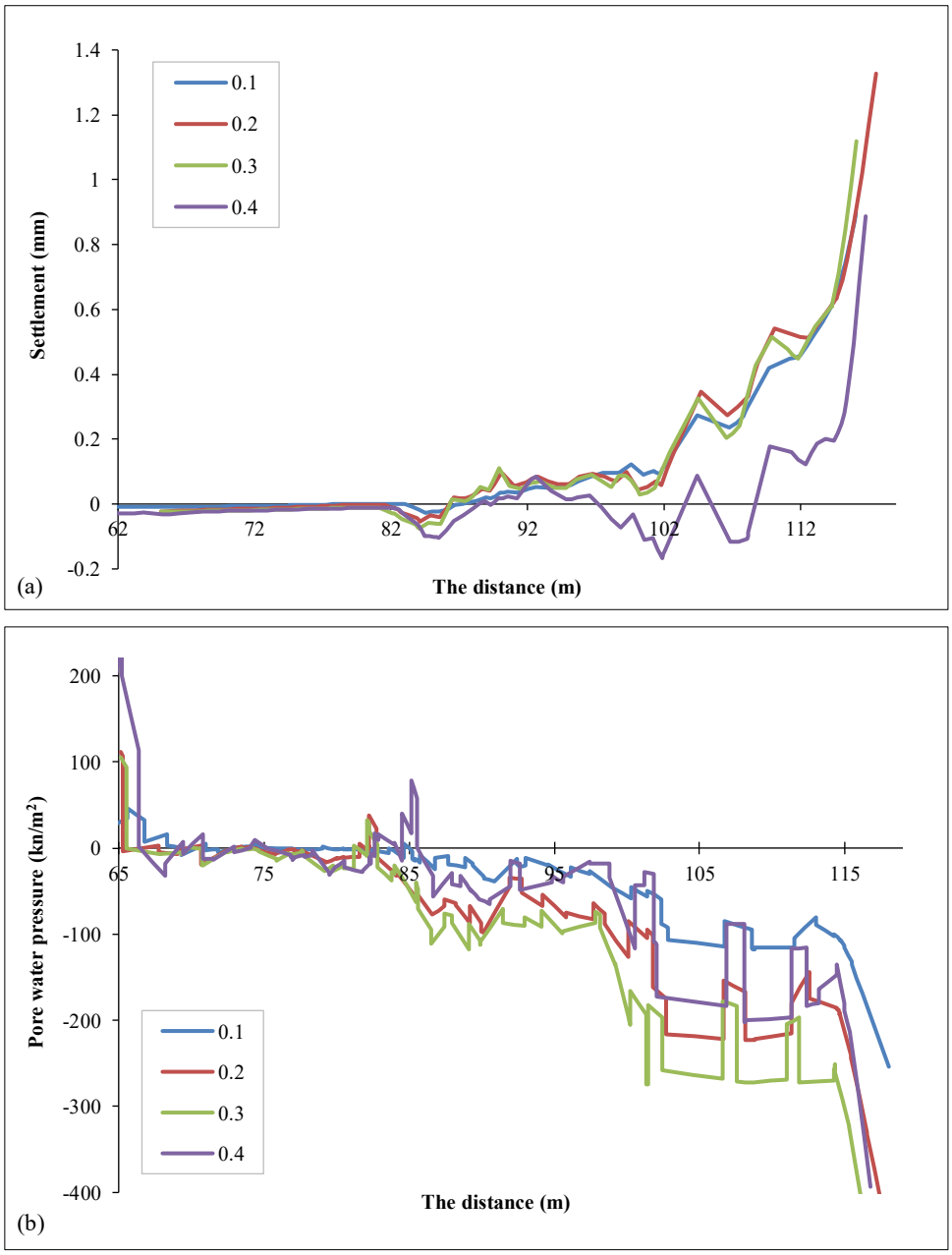

Figure 8. The effect of the rainfall intensity of: (a) The settlement and; (b) The pore water pressure

4.2.2. The Effect of the Rainfall Duration on Fill Slope (High Strength Parameters)

In this section, several rainfall durations were analyzed to evaluate their influence on soil response. The results indicate that when the rainfall duration reached 0.4 days, both the settlement and pore water pressure attained their maximum values. Moreover, at rainfall durations of 0.2 days and 0.3 days, the variations in settlement and pore water pressure were relatively minor, exhibiting nearly identical values. By comparing the two influencing factors—rainfall intensity and rainfall duration—the results reveal that rainfall duration exerts a more significant impact on soil deformation. Prolonged rainfall, however, enables continuous moisture migration, cumulative pore-water pressure buildup, and progressive weakening of the soil structure. Consequently, long-duration rainfall events pose a greater risk to slope stability and tunnel-induced settlement than short-duration, high-intensity storms. For instance, the maximum displacement reached 1.2 mm under a rainfall intensity of 400 mm/day, whereas it increased to 1.9 mm when the rainfall duration extended to 0.4 days, indicating that the duration of rainfall plays a more dominant role in controlling the magnitude of displacement. Figure 9 illustrates the effect of rainfall duration in the settlement and pore water pressure.

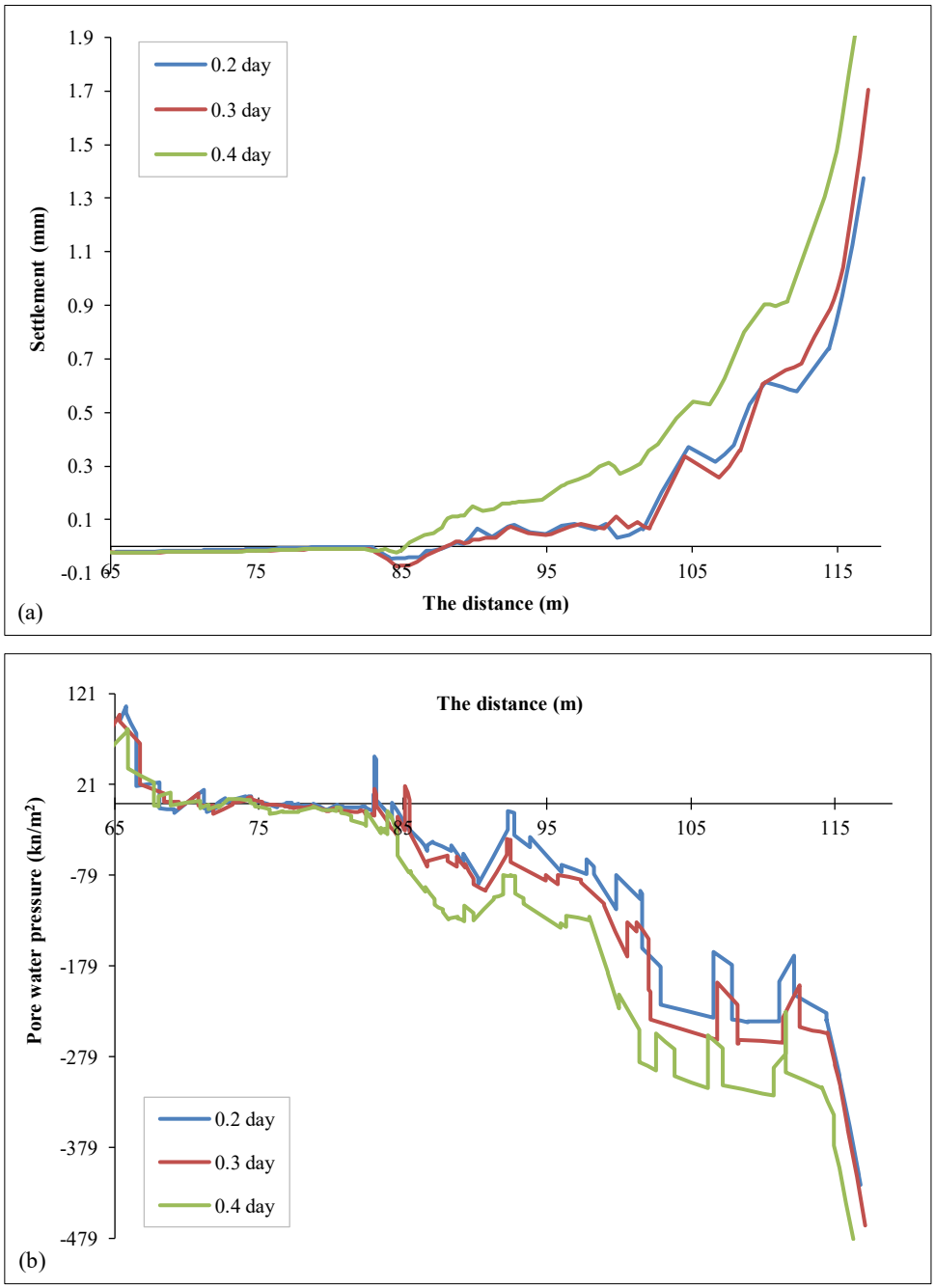

Figure 9. The effect of the rainfall duration on: (a) The displacement and; (b) The pore water pressure

4.2.3. The Behavior under the Effect of Low Parameters

To accurately capture the effect of rainfall on slope stability, the strength parameters of the slope materials were deliberately reduced, as presented in Table 3. Figure 8 illustrates the corresponding factor of safety (FS) values and their spatial distribution. As shown, prior to the reduction of the strength parameters, the FS was approximately 3.6, indicating a stable slope condition. However, after the reduction in shear strength parameters—representing the deterioration of soil strength—the FS decreased to 3.1. This reduction demonstrates the adverse influence of rainfall on slope stability, as the infiltration process leads to softening of the soil mass and a subsequent decline in the overall safety margin. The reduced parameters adopted in the model test and parametric study were determined through a systematic sensitivity analysis rather than arbitrary selection. Key soil parameters, including stiffness and shear strength properties, were progressively reduced within logical and physically realistic ranges reported in previous experimental and numerical studies. The purpose of parameter reduction was to simulate rainfall-induced degradation of soil behavior, such as strength softening and stiffness loss due to increased pore water pressure and reduced effective stress. During the sensitivity analysis, the influence of each reduction level on slope deformation, pore water pressure development, and stability response was evaluated. The selected reduction factors correspond to ranges that produced significant but realistic changes in system response, thereby ensuring that the adopted parameters accurately reflect real soil behavior under adverse hydrological conditions.

However, both figures show similar geometry but slightly different stress or pore-pressure distributions. The color concentration at the upper slope area (red zone) indicates potential plastic deformation or failure initiation.

- Figure 10(a) FS = 3.6, the red/yellow zone is smaller and more localized, suggesting that the soil body still has high resistance and the slope is relatively stable.
- Figure 10(b) FS = 3.1, the red/yellow zone becomes more extended, indicating that a larger part of the slope is reaching the plastic limit, and thus the stability is reduced.

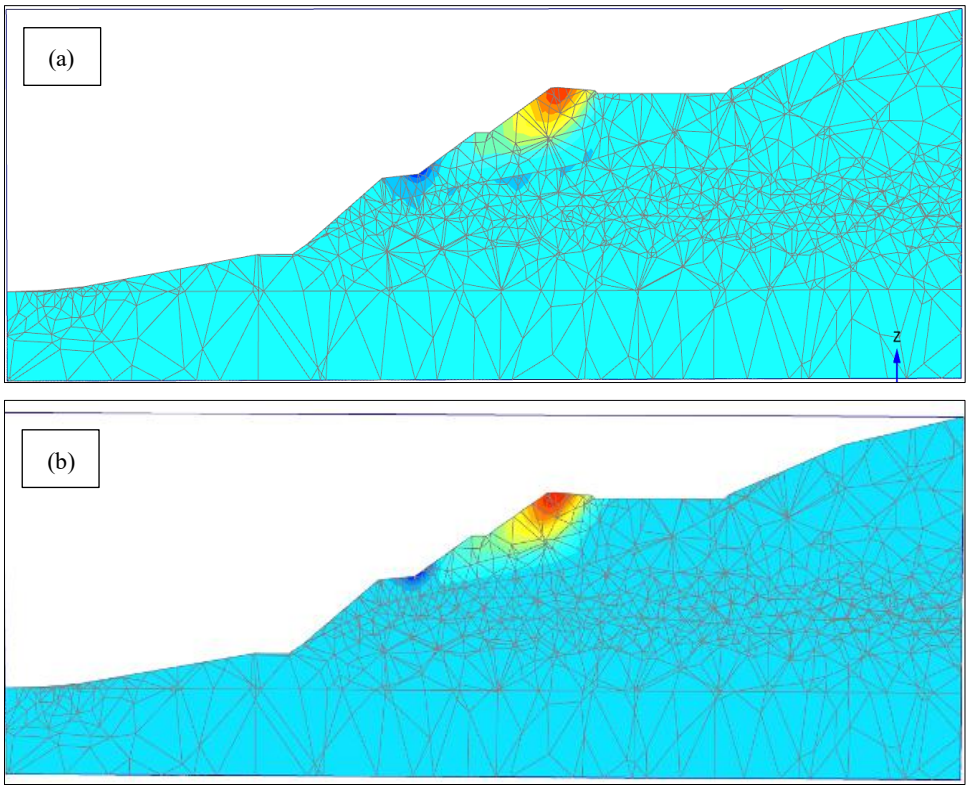

Figure 10. Slope stability without rainfall dry conditions: (a) FS =3.6 and; (b) FS = 3.1

4.2.4. The Proposed Reinforcement Design

Under the condition of reduced material parameters, two primary reinforcement measures were proposed to enhance slope stability. The first reinforcement type consists of piles, which provide deep anchorage and improve the overall load-bearing capacity. The second involves the use of reinforcing plates, which offer surface confinement and contribute to the redistribution of stresses within the slope body. Figure 11 shows the two proposed reinforcement methods.

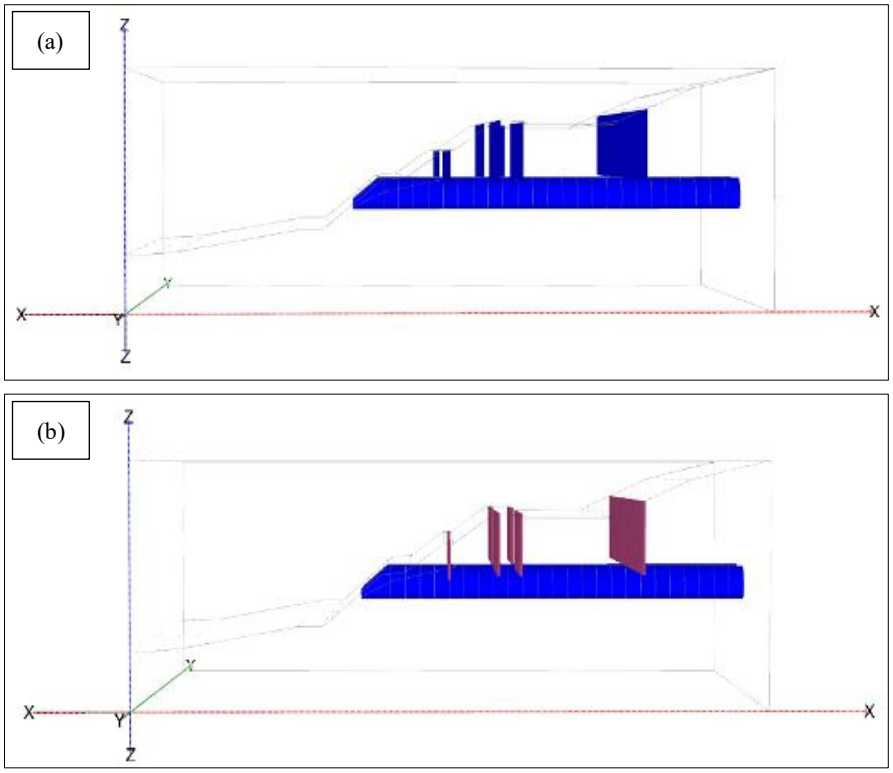

Figure 11. The proposed reinforced models in the numerical simulation: (a) Plates and; (b) Piles

The Piles as Support System

Figure 12(a) presents the displacement response of the slope section under four principal scenarios, each encompassing four specific conditions. The results indicate that the first three scenarios (1) without support, (2) subjected to rainfall without support, and (3) subjected to rainfall with support—exhibit nearly similar displacement patterns, suggesting that the installation of support prior to rainfall does not significantly alter the overall deformation trend. Nevertheless, when the support system is introduced after the rainfall event, the slope demonstrates a noticeable swelling (heaving) behavior instead of settlement. This phenomenon can be attributed to the redistribution of pore water pressure and stress within the soil mass following rainfall infiltration. The subsequent installation of the support structure restricts lateral deformation and vertical settlement, causing an upward movement because of the confined excess pore pressure and the limited drainage pathways within the saturated zone. This behavior highlights the complex interaction between rainfall-induced pore pressure variation and post-rainfall reinforcement timing on slope deformation characteristics.

Figure 12(b) illustrates the saturation distribution within the slope under rainfall conditions. The results indicate that there is no significant difference in the degree of saturation between the supported and unsupported slopes. This suggests that the presence of structural support has a limited influence on the overall infiltration pattern and moisture migration within the slope. The similarity in saturation behavior implies that rainfall infiltration is primarily governed by the soil's hydraulic properties rather than by the mechanical boundary conditions imposed by the support system. From a hydro-mechanical perspective, structural supports such as piles or plates primarily function to redistribute stresses and limit deformation, but they do not substantially modify the soil's pore network or hydraulic conductivity at the slope scale. As a result, rainfall infiltration follows comparable seepage paths in both cases, driven by gravity and capillary forces, leading to similar saturation profiles.

This behavior indicates a decoupling between the hydraulic and mechanical responses of the slope under the investigated conditions, where mechanical reinforcement enhances stability without significantly impeding or redirecting water flow. Previous studies have emphasized that structural reinforcement elements such as piles, soil nails, and plates function primarily as mechanical stabilizers that enhance slope stability through stress redistribution and deformation control, rather than by altering hydraulic conditions within the soil mass. Duncan et al. [25] noted that seepage behavior and moisture migration are generally unaffected by mechanical reinforcement unless specific hydraulic measures, such as drainage systems or impermeable barriers, are incorporated into the design. In the absence of such measures, rainfall infiltration continues to follow the natural seepage paths governed by soil permeability and gravity-driven flow mechanisms. Consequently, mechanical reinforcement can significantly improve slope stability while having a limited influence on infiltration patterns or saturation distribution, which supports the observation that structural support enhances stability without substantially impeding or redirecting water flow.

Figure 12(c) shows the variation of pore water pressure along the slope section under two conditions: rainfall without piles (gray line) and after rainfall with piles (orange line). Overall, the results show that both curves follow a similar trend, but noticeable differences appear at specific sections where the piles are installed. Under the rainfall without piles condition, the pore water pressure remains relatively uniform with moderate fluctuations, reflecting the natural infiltration and drainage behavior of the soil mass. In contrast, after the installation of piles, the pore water pressure distribution becomes more irregular, with localized peaks and drops along the section. This behavior can be attributed to the interaction between the piles and the surrounding soil, which alters the hydraulic conductivity and drainage paths. The piles create zones of stress concentration and reduced permeability, leading to the temporary accumulation of pore pressure near the pile–soil interface.

At the same time, adjacent areas may experience pressure dissipation due to water migration along the structural boundaries. Although the overall saturation distribution remains largely unaffected by the presence of piles, as shown in Figure 12(b), localized variations in pore-water pressure may still occur due to soil–structure interaction. Saturation represents an averaged moisture condition over the slope, whereas pore-water pressure is more sensitive to local changes in permeability and flow paths. Therefore, similar saturation profiles do not necessarily imply uniform pore-pressure distributions, particularly in reinforced slopes where structural elements locally influence seepage behavior. Which means, At the slope scale, the hydraulic response remains largely unchanged; however, at the local scale, soil–structure interaction can induce pore-pressure heterogeneity without altering the overall saturation pattern.

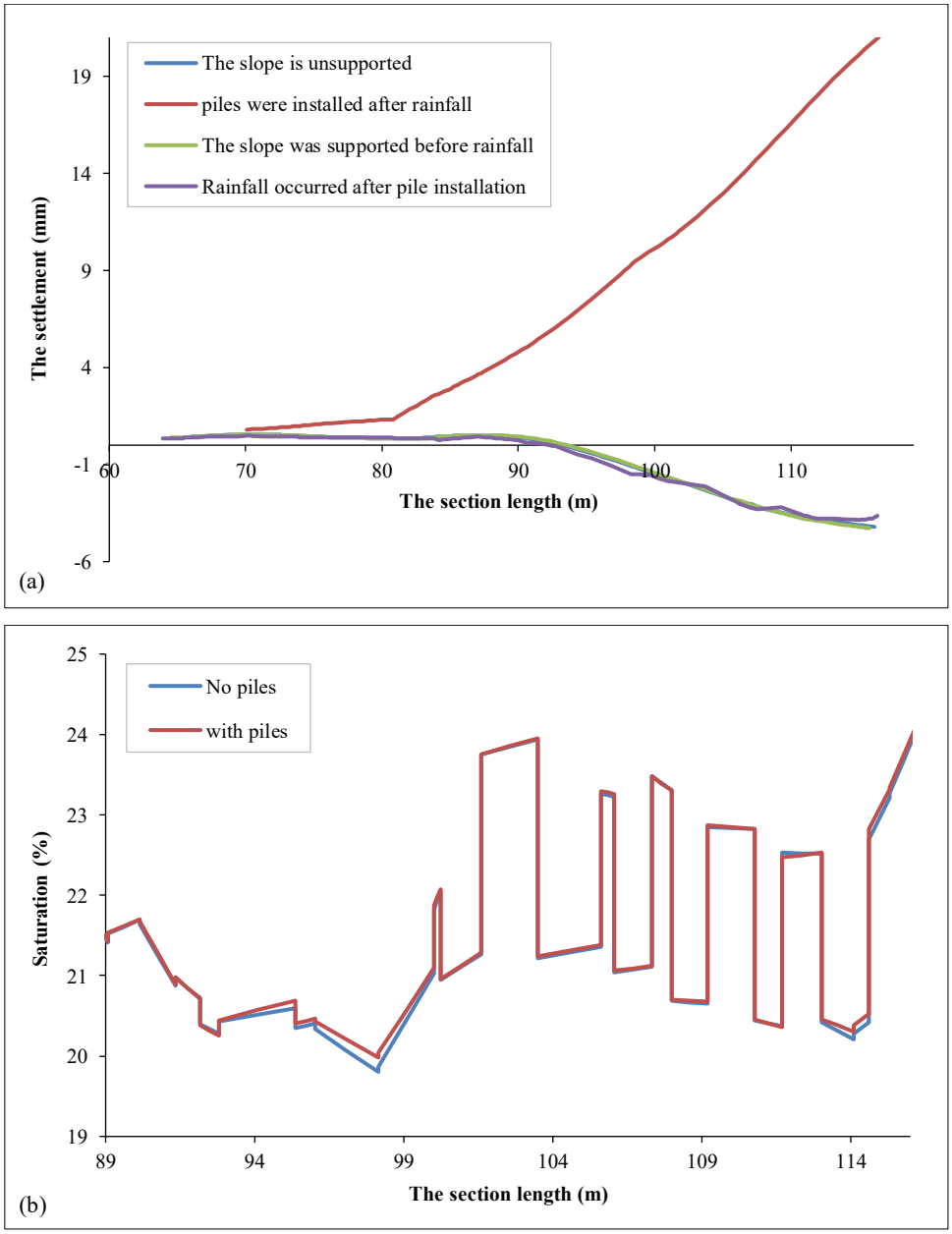

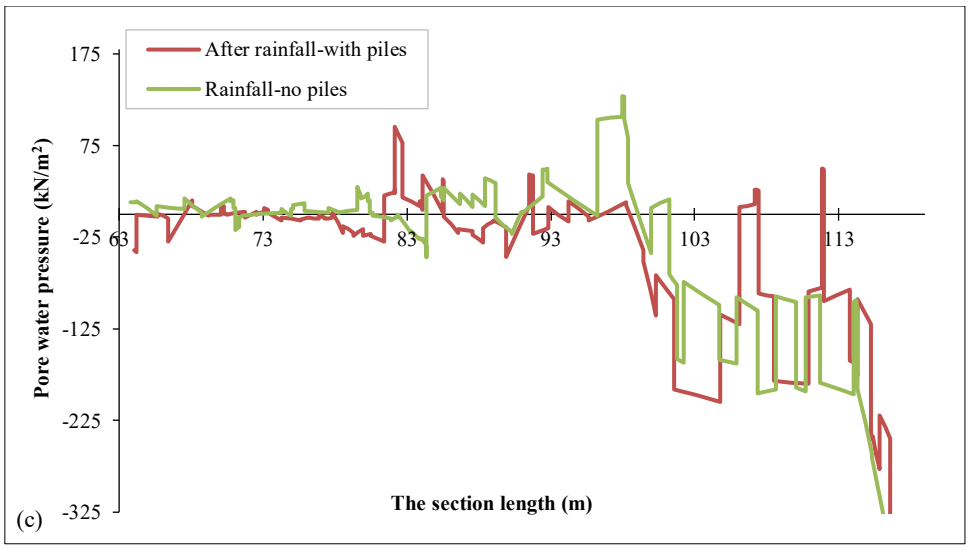

Figure 12. The effect of the support system on the soil parameters piles: (a) The settlement, (b) The saturation, and (c) The pore water pressure

With regard to the factor of safety Figure 13, the results reveal a substantial variation influenced by the timing of pile installation in relation to the rainfall event. Three primary scenarios were analyzed. In the dry condition (without rainfall), the slope exhibited a high level of stability with a factor of safety of FS = 3.3. When rainfall occurred without any supporting system, the factor of safety markedly decreased to FS = 1.3, indicating a significant reduction in stability due to rainfall infiltration and the consequent loss of matric suction within the soil. Conversely, when the rainfall occurred in the presence of installed support, the factor of safety slightly increased to FS = 1.5, demonstrating that the reinforcement contributed to enhancing slope stability by providing additional resistance against deformation and potential failure. These findings emphasize the critical importance of the timing of reinforcement installation, as pre-rainfall support conditions yield improved stability compared with post-rainfall or unsupported conditions. In summary, the correlation between the factor of safety and sustainability highlights that proactive stabilization measures, such as installing piles prior to rainfall, contribute significantly to sustainable slope management. By integrating geotechnical resilience, environmental stewardship, and lifecycle efficiency, such practices ensure that slope reinforcement systems remain safe, durable, and resource-efficient under both ordinary and extreme hydrological conditions.

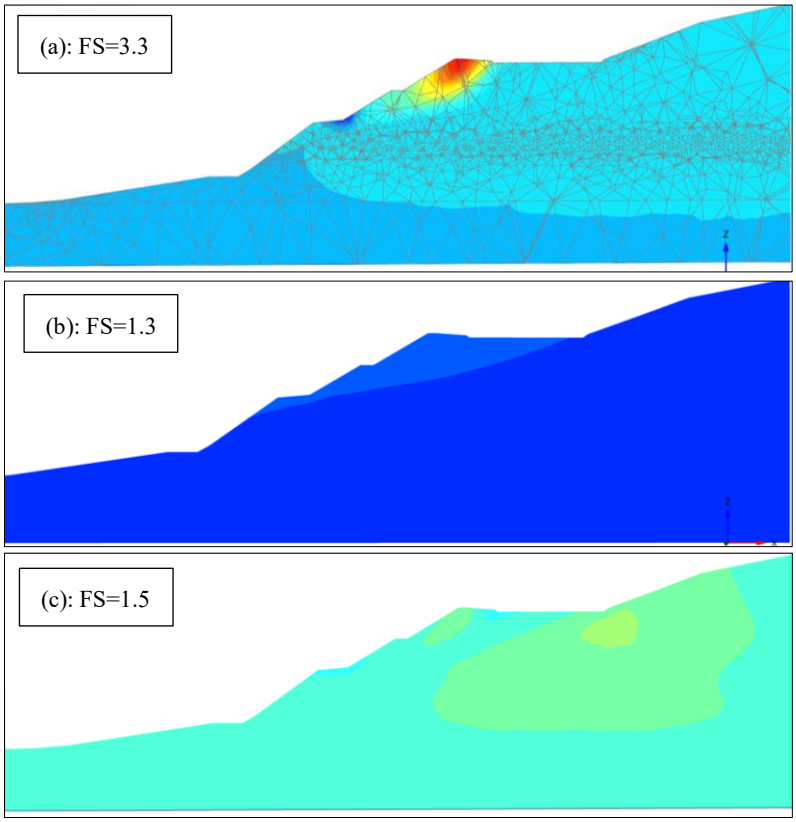

Figure 13. FS before and after the rainfall: (a) The pile installed in the dry condition, (b) the rainfall without support and (c) the pile installed before the rainfall

Plates Support System

In this section, plate elements are employed as a slope support system. Figure 13(a) illustrates the displacement distribution along the inclined portion of the slope under four primary conditions. The first case represents the slope without any support and without rainfall. The second case considers the effect of rainfall in the absence of support. The third case examines the condition of the slope with support but without rainfall. Finally, the fourth case investigates the combined effect of rainfall and support. The results show that the maximum displacement occurred when the slope supported after the rainfall. The reason may be due to the following:

Before the installation of support, the unreinforced slope experiences increased pore water pressure during rainfall infiltration, which reduces the effective stress and leads to softening and downward movement of the soil mass due to gravity. In this condition, deformation primarily occurs in the downward and outward directions as there is no structural restraint to resist the movement. However, after adding support elements such as piles, nails, or retaining walls, the slope gains stiffness and lateral restraint. The reinforcement resists the downward displacement and partially transforms it into upward or lateral reactions. When the boundary conditions are fixed or partially constrained, the compressive forces within the reinforcement can generate upward reaction pressures, resulting in localized heaving or "swelling-type" displacements near the slope face or crest. This phenomenon is mainly attributed to stress redistribution within the slope–support system. The introduction of reinforcement alters the stress path, transferring part of the load from the soil to the structural elements, and in some cases, pushing back against the soil mass. In numerical models such as PLAXIS, this effect is often visible near the interface between the wall and soil due to stiffness contrasts and stress rebalancing during support activation. Additional factors such as initial stress reset, pore pressure dissipation, and boundary or meshing effects may further contribute to the apparent uplift. Overall, after reinforcement, the slope behavior transitions from gravity-driven settlement to a stiffness-controlled equilibrium state, where the restraining action of the support can induce localized upward displacements despite the soil remaining under overall compressive stress.

Figure 13(b) illustrates the variation of excess pore water pressure along the slope section under two conditions: rainfall without support (blue line) and rainfall with support (orange line). The variation of excess pore water pressure along the section shows that both the supported and unsupported slopes experience abrupt changes at specific points, indicating zones of hydraulic or mechanical transition. However, these fluctuations are not synchronized; when the supported case shows a sharp rise or drop, the unsupported case tends to remain relatively stable, and vice versa. This alternating pattern suggests that the presence of support elements alters the local stress–pore pressure interaction rather than uniformly reducing or increasing the pore pressure. In supported slopes, the reinforcement elements constrain the soil deformation and modify the seepage path, causing pressure concentration or dissipation near structural interfaces. In contrast, in the unsupported slope, the absence of such constraints allows a more continuous redistribution of pore pressure, but local zones still show sudden changes due to soil heterogeneity or transient infiltration effects. The lack of synchronization in excess pore-water pressure fluctuations highlights the localized nature of soil–structure interaction under rainfall conditions, where reinforcement alters stress–strain–seepage coupling at specific locations rather than uniformly modifying the hydraulic response of the entire slope. Figure 13(c) which shows the saturation chart shows almost the same results.

Figures 14(c) and 14(b) reveal that pore-water pressure does not increase uniformly along the slope but instead exhibits pronounced spatial variability, with higher peaks occurring mainly in the mid-to-lower slope sections (approximately 100–115 m). From a hydro-mechanical perspective, these peaks result from the convergence of seepage paths driven by gravity, combined with reduced drainage efficiency in zones affected by tunnel excavation and stress redistribution. In the unsupported slope, the absence of structural constraints allows infiltrated rainfall to accumulate more freely, producing higher excess pore-water pressures and sharper pressure gradients. This behavior significantly reduces effective stress and increases the likelihood of deep-seated or progressive failure along potential slip surfaces. By contrast, in the reinforced case, although the global saturation distribution remains similar, soil–structure interaction locally modifies stress transfer and deformation patterns, leading to reduced pore-pressure magnitudes. This indicates that reinforcement primarily mitigates instability by limiting deformation and stress concentration rather than by altering the overall hydraulic regime, thereby shifting the failure mode from global sliding toward more localized deformation.

Figure 15 presents the factor of safety values for the slope under different conditions. The results indicate that the slope was in an unstable condition prior to the installation of support. After rainfall, the factor of safety for the unsupported slope is recorded as 1.15, confirming its susceptibility to failure. However, when support is introduced following rainfall, the factor of safety increases to 1.53, demonstrating a significant improvement in overall stability. This enhancement highlights the effectiveness of the support system in reinforcing the slope, increasing its resistance to deformation and reducing the likelihood of failure under rainfall conditions.

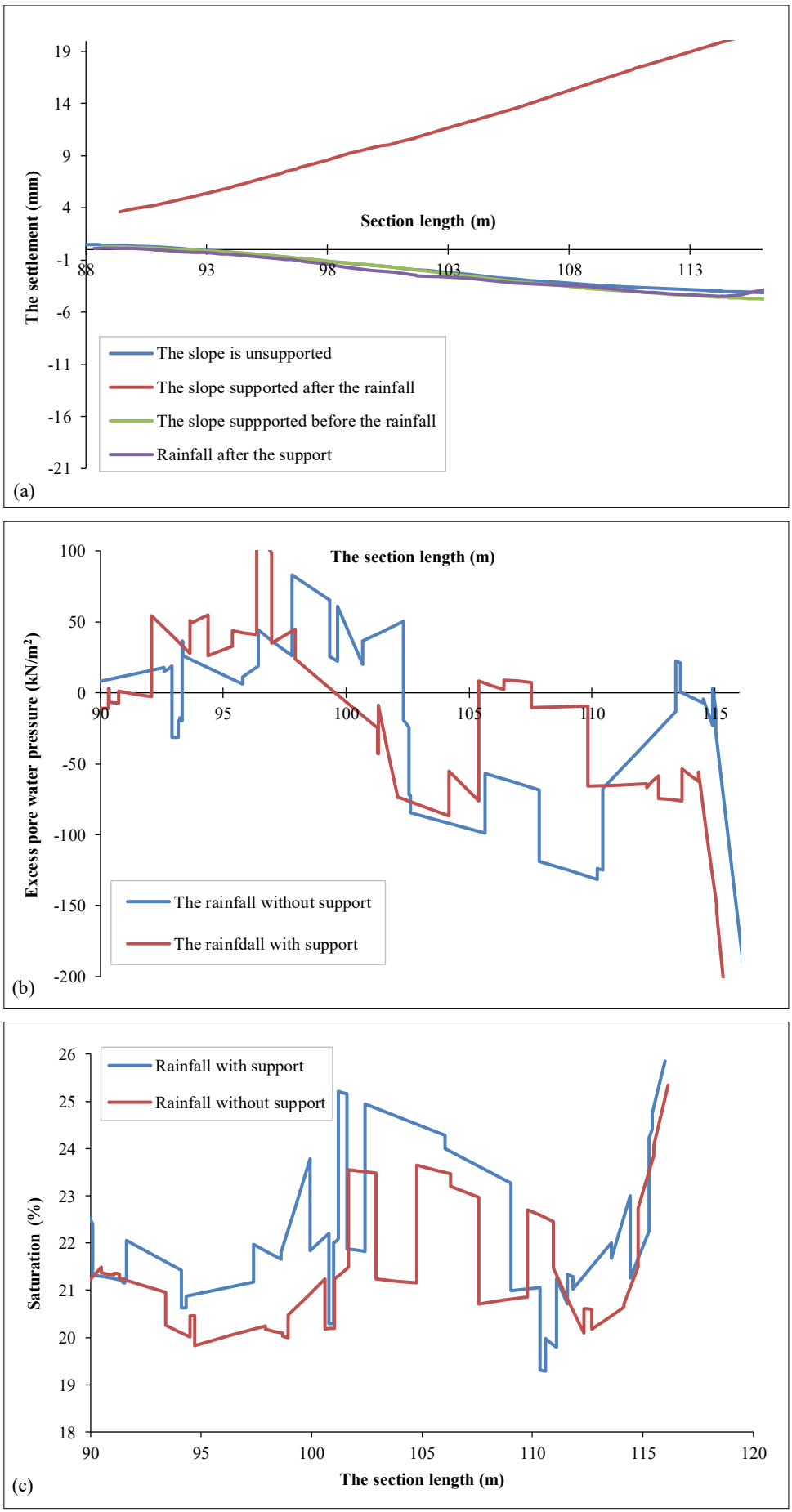

Figure 14. The effect of the support system on the soil parameters plates: (a) The settlement, (b) Pore water pressure and the saturation

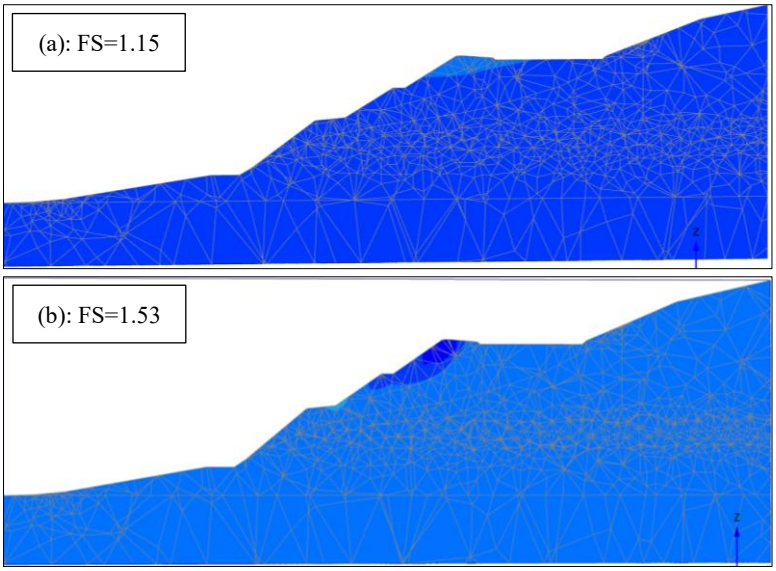

Figure 15. The factor of safety: (a) After the rainfall (No support) and (b) After the rainfall with support

5. Discussion Between the Two Cases

Based on the previous findings, it can be observed that the presence of support structures leads to a higher flow rate compared with the unsupported condition. In the section, which is located between the two tunnels, when there is a support system, the total discharge is 16.95 m³/day. While, when there is no support, the total discharge is 7 m³/day as shown in Figure 16. The same happened for the plates as shown in Figure 17. When there are plates, the total discharge is 8.8 m³/day. While when there is no support, the total discharge is 7 m³/day. This phenomenon can be attributed to the alteration of hydraulic pathways within the slope caused by the installation of structural elements such as piles or retaining systems. In other words:

This behavior can be explained by the difference in hydraulic pathways and pore pressure distribution induced by the presence or absence of structural support within the slope. When support is installed, the structural elements (e.g., piles, retaining plates, or slabs) create preferential flow channels and localized stress concentrations at the soil–structure interfaces. These interfaces often contain micro-gaps or less compacted zones that facilitate water movement, resulting in higher seepage flow rates. Additionally, the installation of support alters the natural drainage pattern by redirecting infiltrated water along the structural boundaries, thereby increasing the overall measured flow. In contrast, when no support is present, the slope remains as a homogeneous and more compacted soil mass, which resists rapid water percolation. The absence of artificial interfaces or stress discontinuities limits the permeability and reduces the hydraulic conductivity of the slope system. Consequently, the infiltrated rainfall tends to move more slowly through the soil matrix, leading to a lower overall flow rate. In summary, the higher flow in the supported slope is primarily attributed to the formation of preferential seepage paths and altered hydraulic gradients induced by the support installation, whereas the lower flow in the unsupported slope results from the more uniform and less permeable soil structure that restricts water migration.

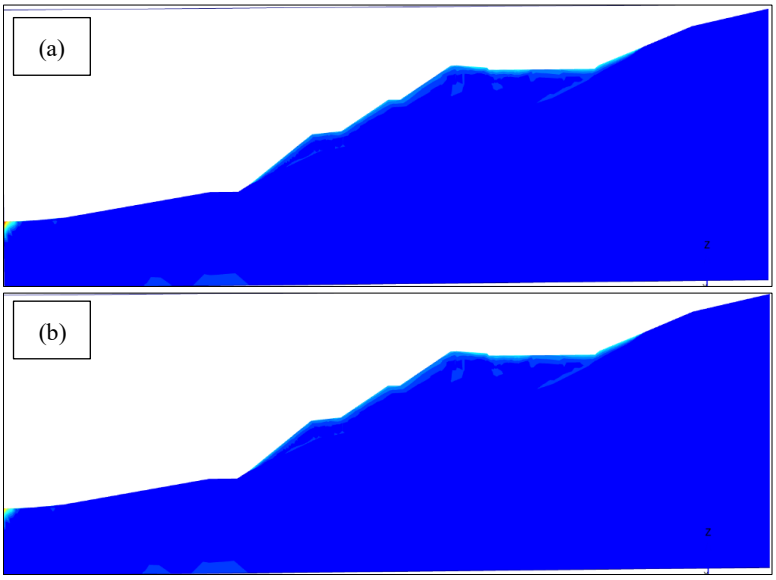

Figure 16. The rainfall flow diagram: (a) Piles with a support system and (b) Piles without support

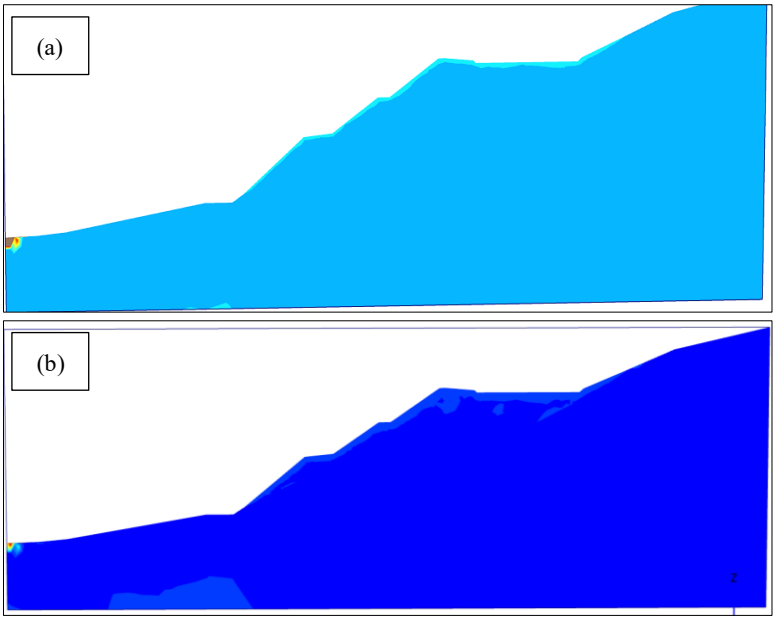

Figure 17. The rainfall flow diagram: (a) Plates with support and (b) Plates without support

6. Conclusion

This study investigated ground settlement and slope deformation induced by the excavation of twin parallel tunnels within a slope, with particular emphasis on the coupled effects of rainfall infiltration and reinforcement measures. The numerical results obtained from the finite element method (FEM) showed strong agreement with the physical model tests, confirming the robustness and reliability of the adopted numerical framework. The consistency between experimental observations and simulations demonstrates that the Mohr–Coulomb constitutive model is adequate for capturing the mechanical behavior of the slope material under both dry and rainfall conditions in this case. The analysis further confirms that tunnel excavation significantly alters stress redistribution within the slope, leading to measurable surface settlement and localized deformation zones, which are further amplified when rainfall is introduced.

A key finding of this research is that rainfall duration plays a more critical role in slope deformation than rainfall intensity. While increases in rainfall intensity beyond 300 mm/day result in elevated pore-water pressure and limited additional settlement, prolonged rainfall duration (up to 0.4 days) produces substantially greater displacement and pore pressure accumulation. This highlights that long-duration rainfall events pose a higher risk to slope stability due to sustained saturation, reduction in matric suction, and progressive loss of effective stress. In addition, the study reveals that reinforcement systems, including piles and plates, influence not only the mechanical response but also the hydraulic behavior of the slope. Reinforced slopes exhibited higher total seepage discharge than unsupported slopes, attributed to the development of preferential flow paths along soil–structure interfaces. This finding underscores the importance of integrating hydraulic considerations into reinforcement design, particularly under rainfall conditions. Overall, the results demonstrate that timely reinforcement combined with advanced numerical modeling can significantly enhance the resilience of tunnel-affected slopes under extreme rainfall. Future research should focus on fully coupled rainfall–reinforcement interaction models and long-term field monitoring to better assess slope performance under changing climatic conditions.

7. Symbols

C_1	Similarity Ratio	C	Cohesion
E	Modulus of Elasticity	Phi	Friction angle
μ	Poisson ratio	γ	Unit weight
d	Pile diameter	t	Plate thickness

8. Declarations

8.1. Author Contributions

Conceptualization, Z.A. and L.S.; methodology, Z.A. and L.S.; software, L.S. and Z.A.; validation, L.S. and H.A. and Z.A.; formal analysis L.S.; investigation, Z.A. and L.S.; resources, L.S. and H.A.; data curation, L.S. and Z.A.; writing—original draft preparation, L.S. and Z.A.; writing—review and editing, Z.A., L.S., H.A., and A.A.; visualization, L.S. and A.A.; supervision, L.S. and Z.A.; project administration, Z.A. and L.S. All authors have read and agreed to the published version of the manuscript.

8.2. Data Availability Statement

The data presented in this study are available on request from the corresponding author.

8.3. Funding and Acknowledgments

The authors extend their appreciation to Prince Sattam bin Abdulaziz University for funding this research work through the project number (PSAU/2025/01/35302). The PLAXIS 3D v2025.1 analyses used in this study were performed by GeoStruXer Constructs, whose technical support is gratefully acknowledged.

8.4. Conflicts of Interest

The authors declare no conflict of interest.

9. References

[1] Hwang, J., & Lall, U. (2024). Increasing dam failure risk in the USA due to compound rainfall clusters as climate changes. Npj Natural Hazards, 1(1), 27. doi:10.1038/s44304-024-00027-6.

[2] Xie, C., Xu, C., Huang, Y., Liu, J., Shao, X., Xu, X., Gao, H., Ma, J., & Xiao, Z. (2025). Advances in the study of natural disasters induced by the "23.7" extreme rainfall event in North China. Natural Hazards Research, 1, 1–13. doi:10.1016/j.nhres.2025.01.003.

[3] Zhuang, Y., Hu, X., He, W., Shen, D., & Zhu, Y. (2024). Stability Analysis of a Rocky Slope with a Weak Interbedded Layer under Rainfall Infiltration Conditions. Water (Switzerland), 16(4), 604. doi:10.3390/w16040604.

[4] Tian, C., Xiao, Z., Ye, F., Tong, Y., Cao, X., Sun, J., & Li, Z. (2025). The impact of extreme rainfall and drainage system failure on rock tunnels: A case study of deep-buried karst tunnel. Engineering Failure Analysis, 171, 109345. doi:10.1016/j.engfailanal.2025.109345.

[5] Tang, K., Liu, D., Xie, S., Qiu, J., Lai, J., Liu, T., & Fang, Y. (2024). Analysis of loess water migration regularity and failure response of tunnel structure under rainfall environment. Bulletin of Engineering Geology and the Environment, 83(6), 251. doi:10.1007/s10064-024-03715-9.

[6] Qian, W., Tang, X., Ma, X., & Wang, X. (2025). Mechanical Characteristics and Safety Evaluation of Tunnel Lining Structures in Karst Areas Under Heavy Rainfall Conditions. Buildings, 15(10), 1756. doi:10.3390/buildings15101756.

[7] Xu, S., Lei, H., Li, C., Liu, H., Lai, J., & Liu, T. (2021). Model test on mechanical characteristics of shallow tunnel excavation failure in gully topography. Engineering Failure Analysis, 119, 104978. doi:10.1016/j.engfailanal.2020.104978.

[8] Jiang, X., Wang, F., Yang, H., & Niu, J. (2018). Parameter Sensitivity of Shallow-Bias Tunnel with a Clear Distance Located in Rock. Advances in Civil Engineering, 5791354. doi:10.1155/2018/5791354.

[9] Choi, J. I., & Lee, S. W. (2010). Influence of Existing Tunnel on Mechanical Behavior of New Tunnel. KSCE Journal of Civil Engineering, 14(5), 773–783. doi:10.1007/s12205-010-1013-8.

[10] Kim, J.-W. (2012). A Study on the Stability of Asymmetrical Twin Tunnels in Alternating Rock Layers Using Scaled Model Tests. Journal of Korean Society for Rock Mechanics, 22(1), 22–31. doi:10.7474/tus.2012.22.1.022.

[11] Seo, H. J., Choi, H., Lee, K. H., Bae, G. J., & Lee, I. M. (2014). Pillar-reinforcement technology beneath existing structures: Small-scale model tests. KSCE Journal of Civil Engineering, 18(3), 819–826. doi:10.1007/s12205-014-1392-3.

[12] Ng, C. W. W., & Lu, H. (2014). Effects of the construction sequence of twin tunnels at different depths on an existing pile. Canadian Geotechnical Journal, 51(2), 173–183. doi:10.1139/cgj-2012-0452.

[13] Chen, R. P., Lin, X. T., Kang, X., Zhong, Z. Q., Liu, Y., Zhang, P., & Wu, H. N. (2018). Deformation and stress characteristics of existing twin tunnels induced by close-distance EPBS under-crossing. Tunnelling and Underground Space Technology, 82, 468–481. doi:10.1016/j.tust.2018.08.059.

[14] Zhao, W., Jia, P. J., Zhu, L., Cheng, C., Han, J., Chen, Y., & Wang, Z. Guo. (2019). Analysis of the additional stress and ground settlement induced by the construction of double-O-tube shield tunnels in sandy soils. Applied Sciences (Switzerland), 9(7), 1399. doi:10.3390/app9071399.

[15] Zhu, Z. G., Huang, S., & Zhu, Y. Q. (2012). Study of road surface settlement rule and controlled criterion for railway tunnel undercrossing highway. Yantu Lixue/Rock and Soil Mechanics, 33(2), 558.

[16] Song, Z., Mao, J., Tian, X., Zhang, Y., & Wang, J. (2019). Optimization analysis of controlled blasting for passing through houses at close range in super-large section tunnels. Shock and Vibration, 1941436. doi:10.1155/2019/1941436.

[17] Kaya, A., Akgün, A., Karaman, K., & Bulut, F. (2016). Understanding the mechanism of slope failure on a nearby highway tunnel route by different slope stability analysis methods: a case from NE Turkey. Bulletin of Engineering Geology and the Environment, 75(3), 945–958. doi:10.1007/s10064-015-0770-5.

[18] Fattah, M. Y., Shlash, K. T., & Salim, N. M. (2013). Prediction of settlement trough induced by tunneling in cohesive ground. Acta Geotechnica, 8(2), 167–179. doi:10.1007/s11440-012-0169-4.

[19] Lin, H., & Zhong, W. (2019). Influence of Rainfall Intensity and Its Pattern on the Stability of Unsaturated Soil Slope. Geotechnical and Geological Engineering, 37(2), 615–623. doi:10.1007/s10706-018-0631-7.

[20] Ma, K. C., Tan, Y. C., & Chen, C. H. (2011). The influence of water retention curve hysteresis on the stability of unsaturated soil slopes. Hydrological Processes, 25(23), 3563–3574. doi:10.1002/hyp.8081.

[21] Tu, G. xiang, Huang, D., & Deng, H. (2019). Reactivation of a huge ancient landslide by surface water infiltration. Journal of Mountain Science, 16(4), 806–820. doi:10.1007/s11629-018-5315-5.

[22] Rahardjo, H., Ong, T. H., Rezaur, R. B., & Leong, E. C. (2007). Factors Controlling Instability of Homogeneous Soil Slopes under Rainfall. Journal of Geotechnical and Geoenvironmental Engineering, 133(12), 1532–1543. doi:10.1061/(asce)1090-0241(2007)133:12(1532).

[23] Ng, C. W. W., & Shi, Q. (1998). A Numerical Investigation of the Stability of Unsaturated Soil Slopes Subjected to Transient Seepage. Computers and Geotechnics, 22(1), 1–28. doi:10.1016/S0266-352X(97)00036-0.

[24] Fredlund, D. G., & Rahardjo, H. (2025). Soil Mechanics for Unsaturated Soils. Soil Mechanics for Unsaturated Soils. John Wiley & Sons, New Jersey, United States. doi:10.1002/9780470172759.

[25] Duncan, J. M., Wright, S. G., & Brandon, T. L. (2014). Soil strength and slope stability. Wiley, New Jersey, United States.